ACADEMIC PRESS

Available online at www.sciencedirect.com
SCIENCE DIRECT®

Journal of Solid State Chemistry 174 (2003) 19–31

JOURNAL OF SOLID STATE CHEMISTRY

http://elsevier.com/locate/jssc

Synthesis, crystal structure and electrical characterization of two new potassium uranyl molybdates $K_2(UO_2)_2(MoO_4)O_2$ and $K_8(UO_2)_8(MoO_5)_3O_6$

S. Obbade,[a,*] S. Yagoubi,[a] C. Dion,[a] M. Saadi,[b] and F. Abraham[a]

[a] *Laboratoire de Cristallochimie et Physicochimie du Solide, UMR CNRS 8012, ENSCL-USTL, BP 108, 59652 Villeneuve d'Ascq Cedex, France*
[b] *Laboratoire de Chimie de Coordination et Analytique, Faculté des Sciences, Université Chouaib Doukkali, B.P. 20 El Jadida, Morocco*

Received 20 December 2002; received in revised form 28 February 2003; accepted 8 March 2003

Abstract

Two new potassium uranyl molybdates $K_2(UO_2)_2(MoO_4)O_2$ and $K_8(UO_2)_8(MoO_5)_3O_6$ have been obtained by solid state chemistry . The crystal structures were determined by single crystal X-ray diffraction data, collected with Mo$K\alpha$ radiation and a charge coupled device (CCD) detector. Their structures were solved using direct methods and Fourier difference techniques and refined by a least square method on the basis of F^2 for all unique reflections, with $R_1 = 0.046$ for 136 parameters and 1412 reflections with $I \geqslant 2\sigma(I)$ for $K_2(UO_2)_2(MoO_4)O_2$ and $R_1 = 0.055$ for 257 parameters and 2585 reflections with $I \geqslant 2\sigma(I)$ for $K_8(UO_2)_8(MoO_5)_3O_6$. The first compound crystallizes in the monoclinic symmetry, space group $P2_1/c$ with $a = 8.250(1)$ Å, $b = 15.337(2)$ Å, $c = 8.351(1)$ Å, $\beta = 104.75(1)^\circ$, $\rho_{mes} = 5.22(2)$ g/cm^3, $\rho_{cal} = 5.27(2)$ g/cm^3 and $Z = 4$. The second material adopts a tetragonal unit cell with $a = b = 23.488(3)$ Å, $c = 6.7857(11)$ Å, $\rho_{mes} = 5.44(3)$ g/cm^3, $\rho_{cal} = 5.49(2)$ g/cm^3, $Z = 4$ and space group $P4/n$.

In both structures, the uranium atoms adopt a UO_7 pentagonal bipyramid environment, molybdenum atoms are in a MoO_4 tetrahedral environment for $K_2(UO_2)_2(MoO_4)O_2$ and MoO_5 square pyramid coordination in $K_8(UO_2)_8(MoO_5)_3O_6$. These compounds are characterized by layered structures. The association of uranyl ions (UO_7) and molybdate oxoanions MoO_4 or MoO_5, give infinite layers $[(UO_2)_2(MoO_4)O_2]^{2-}$ and $[(UO_2)_8(MoO_5)_3O_6]^{8-}$ in $K_2(UO_2)_2(MoO_4)O_2$ and $K_8(UO_2)_8(MoO_5)_3O_6$, respectively. Conductivity properties of alkali metal within the interlayer spaces have been measured and show an Arrhenius type evolution.

Keywords: Uranyl molybdates; Crystal structure; Layered structure; Ionic conductivity

1. Introduction

Independently of the mineralogical aspect and ecological interest in storage of spent nuclear fuel, alkali and transition metal uranyl oxides, and particularly alkali uranyl molybdates are presenting an important structural interest because of their structural diversity [1], related to the numerous coordination possibilities of Mo^{VI} ion with tetrahedral, octahedral, square pyramidal and 5-fold triangular bipyramidal coordination, the two latter being more uncommon. Moreover, in uranyl containing oxides, various types of layered structures are often observed that represent an additional interest because these structures are generally favorable for a good cationic electrical conductivity due to the mobility of the monovalent cations between the formed layers, as in HUP [2] and BIMEVOX materials [3].

In the homogeneous family of anhydrous compounds with formula UO_2XO_4, X = S, Se, Cr, Mo and W in the higher bond valence X^{VI}, the crystal structure can be described by the association of XO_4^{2-} tetrahedra with $[UO_2(O_5)]^{2+}$ pentagonal bipyramids [3–7], where each XO_4^{2-} tetrahedron shares its corners with four neighboring uranium bipyramids to form a three-dimensional framework. Such tetrahedra were also observed in anhydrous alkali mono-molybdates M_2MoO_4 (M = Na, K) [8,9], and in numerous alkali uranyl molybdates such as $M_2(UO_2)(MoO_4)_2$ (M = Na, K, Rb) [10–12], and $K_2(UO_2)(MoO_4)_2 \cdot 2H_2O$ [11] obtained by the combination of UO_2MoO_4 and M_2MoO_4, in ratio 1/1.

In the structures of umohoïte $[(UO_2)MoO_4(H_2O)]\cdot H_2O$ [13] and iriginite $[UO_2Mo_2O_7(H_2O)_2](H_2O)$ [14,15], Mo^{VI} ions are in a strongly distorted octahedral

*Corresponding author. Fax: +33-320-436-814.
E-mail address: obbade@ensc-lille.fr (S. Obbade).

0022-4596/03/$ - see front matter © 2003 Elsevier Science (USA). All rights reserved.
doi:10.1016/S0022-4596(03)00168-3

Table 1
Observed and calculated X-ray powder diffraction pattern for $K_2(UO_2)_2(MoO_4)O_2$

h	k	l	$2\theta_{obs}$	$2\theta_{cal}$	I (%)	h	k	l	$2\theta_{obs}$	$2\theta_{cal}$	I (%)
1	0	0	11.07	11.08	100	3	3	0	38.11	38.10	5
0	2	0	11.52	11.53	23	3	3	−2	39.56	39.58	1
0	1	1	12.36	12.37	3	2	3	2	39.64	39.65	1
1	1	0	12.48	12.49	70	1	4	−3	40.06	40.05	1
0	2	1	15.92	15.91	6	2	5	−2	40.14	40.15	3
1	2	0	16.00	16.01	65	1	5	2	40.20	40.19	1
0	3	1	20.54	20.53	3	1	6	−2	41.74	41.76	1
1	3	0	20.60	20.61	35	3	4	−2	42.65	42.66	1
1	0	−2	21.96	21.94	2	1	0	−4	43.24	43.24	11
1	1	−2	22.72	22.71	9	4	1	−1	44.25	44.24	1
0	1	2	22.72	22.73	4	0	5	3	44.73	44.72	1
2	1	0	23.02	23.01	2	2	0	−4	44.76	44.75	4
1	2	−2	24.84	24.85	10	0	0	4	44.81	44.80	4
0	2	2	24.86	24.88	7	1	4	3	44.85	44.84	4
2	2	0	25.14	25.13	2	2	6	−2	44.87	44.85	5
0	4	1	25.68	25.69	5	1	6	2	44.89	44.89	7
1	4	0	25.73	25.75	9	1	2	−4	44.92	44.90	3
1	4	−1	26.87	26.88	2	2	6	1	45.02	45.01	1
2	0	−2	27.05	27.07	21	1	7	1	45.04	45.03	1
1	0	2	27.15	27.13	28	3	5	0	45.05	45.07	7
2	1	−2	27.68	27.70	4	2	1	−4	45.18	45.16	2
1	1	2	27.77	27.76	7	4	0	−2	45.22	45.21	2
2	1	1	27.92	27.93	3	0	1	4	45.23	45.21	1
1	3	−2	28.09	28.10	50	4	0	0	45.42	45.41	7
0	3	2	28.11	28.12	24	4	2	−1	45.46	45.47	1
2	3	0	28.33	28.34	90	4	1	−2	45.60	45.61	1
2	2	−2	29.53	29.51	6	3	1	2	45.72	45.71	2
1	2	2	29.55	29.57	9	2	5	−3	46.19	46.18	1
2	2	1	29.74	29.73	2	3	5	−2	46.35	46.37	2
0	5	1	31.15	31.16	2	2	2	−4	46.36	46.37	4
1	5	0	31.22	31.21	7	0	2	4	46.41	46.42	2
1	4	−2	32.14	32.13	4	2	5	2	46.42	46.43	3
2	4	−1	32.29	32.28	2	2	2	3	46.73	46.72	1
2	3	−2	32.31	32.32	2	4	2	−2	46.82	46.81	3
1	1	−3	32.73	32.74	2	3	2	2	46.92	46.91	3
3	0	0	33.65	33.66	4	4	2	0	47.03	47.01	2
0	1	3	33.73	33.74	2	2	7	−1	47.24	47.23	1
3	1	0	34.15	34.17	5	0	8	0	47.36	47.37	2
0	6	0	35.09	35.07	12	2	3	−4	48.31	48.33	3
3	0	−2	35.32	35.30	5	1	6	−3	48.33	48.35	3
2	0	2	35.36	35.38	7	1	5	3	48.40	48.42	1
3	2	0	35.67	35.69	7	3	6	−1	48.63	48.64	2
2	1	2	35.87	35.88	2	3	5	1	48.71	48.70	2
1	5	−2	36.73	36.73	7	0	8	1	48.76	48.77	5
0	5	2	36.74	36.75	2	4	3	−2	48.76	48.77	5
2	5	−1	36.85	36.86	2	1	8	0	48.82	48.81	5
1	6	0	36.90	36.89	4	3	3	2	48.84	48.85	10
2	5	0	36.94	36.93	11	4	3	0	48.94	48.96	1
2	2	−3	37.01	37.03	2	3	6	0	49.38	49.40	5
3	2	−2	37.24	37.25	2	2	7	−2	49.94	49.96	1
2	2	2	37.32	37.33	13	1	7	2	49.98	50.00	1

$a = 8.2558(2)$, $b = 15.3395(4)$, $c = 8.3621(2)$ and $\beta = 104.801(2)$ with $F_{20} = 52$ (0.0125, 31).

coordination involving five oxygen atoms and one H_2O group, where MoO_6 octahedra and UO_7 pentagonal bipyramids are associated to form neutral layers linked together via hydrogen bonds involving interlayer H_2O groups. This coordination of molybdenum has also been observed in tetramolybdate $K_2Mo_4O_{13}$ [16], where the structure consists of infinite chains built up from edge-shared MoO_6 octahedra, the chains being held together by interleaving K ions. In dimolybdates $M_2Mo_2O_7$ (M = Na, K) [17,18], the structure is formed by the association of MoO_6 octahedra and MoO_4 tetrahedra. The crystal structure of these compounds is built from $(MoO_5)_\infty$ infinite chains of MoO_6 octahedra sharing opposite corners and MoO_4 tetrahedra bridging

Table 2
Observed and calculated X−ray powder diffraction pattern for $K_8(UO_2)_8(MoO_5)_3O_6$

h	k	l	$2\theta_{obs}$	$2\theta_{cal}$	I (%)	h	k	l	$2\theta_{obs}$	$2\theta_{cal}$	I (%)
2	2	0	10.67	10.66	2	5	7	0	32.83	32.82	4
0	0	1	13.05	13.04	100	2	5	2	33.45	33.46	5
0	1	1	13.57	13.58	96	1	8	1	33.47	33.49	2
1	1	1	14.11	14.09	15	4	4	2	34.14	34.13	5
0	2	1	15.09	15.07	7	2	8	1	34.15	34.16	3
0	4	0	15.09	15.09	5	4	8	0	34.15	34.16	1
1	2	1	15.53	15.54	4	3	5	2	34.58	34.57	10
3	3	0	16.01	16.02	4	1	9	0	34.62	34.60	1
2	2	1	16.86	16.87	2	5	7	1	35.44	35.45	2
2	4	0	16.88	16.89	2	2	6	2	35.85	35.85	1
0	3	1	17.28	17.29	1	4	5	2	36.05	36.06	2
1	3	1	17.72	17.71	2	3	6	2	36.92	36.90	2
2	3	1	18.88	18.89	3	0	9	1	36.92	36.92	1
0	4	1	20.01	20.00	2	1	9	1	37.13	37.12	1
3	3	1	20.73	20.71	1	0	7	2	37.73	37.71	3
3	5	0	22.06	22.08	5	2	9	1	37.72	37.73	1
0	6	0	22.75	22.73	15	3	9	1	38.72	38.73	2
0	5	1	23.02	23.03	3	3	7	2	39.51	39.49	1
2	6	0	23.96	23.98	14	4	9	1	40.10	40.10	2
2	5	1	24.25	24.27	7	1	2	3	40.80	40.80	5
4	4	1	25.17	25.15	5	1	8	2	40.83	40.84	2
3	5	1	25.72	25.73	20	1	10	1	40.85	40.86	1
0	0	2	26.24	26.26	6	2	2	3	41.36	41.36	4
0	6	1	26.28	26.29	10	2	8	2	41.42	41.40	2
0	1	2	26.56	26.54	4	2	10	1	41.42	41.42	1
1	6	1	26.59	26.57	11	5	9	1	41.79	41.79	1
1	1	2	26.80	26.81	20	2	3	3	42.28	42.29	4
1	7	0	26.84	26.86	12	3	8	2	42.32	42.33	5
0	2	2	27.35	27.35	29	3	10	1	42.36	42.35	3
2	6	1	27.38	27.39	15	2	4	3	43.58	43.56	3
4	6	0	27.42	27.40	7	4	8	2	43.62	43.59	5
1	2	2	27.60	27.62	10	4	10	1	43.63	43.62	5
4	5	1	27.64	27.65	11	8	8	0	43.63	43.62	2
2	2	2	28.40	28.41	4	0	9	2	43.79	43.77	1
0	3	2	28.69	28.67	17	6	9	1	43.79	43.80	4
3	6	1	28.72	28.70	4	1	9	2	43.94	43.95	2
1	3	2	28.94	28.93	4	3	11	0	43.99	43.98	3
3	7	0	28.99	28.96	4	0	5	3	44.44	44.45	4
2	3	2	29.67	29.69	5	2	9	2	44.49	44.48	5
0	7	1	29.70	29.71	5	0	11	1	44.52	44.50	5
1	7	1	29.95	29.96	8	1	11	1	44.68	44.68	1
0	4	2	30.42	30.43	4	6	10	0	45.04	45.04	4
4	6	1	30.46	30.45	2	5	8	2	45.19	45.18	1
1	4	2	30.65	30.67	2	2	11	1	45.20	45.21	2
3	3	2	30.93	30.91	2	3	9	2	45.36	45.36	2
2	4	2	31.37	31.39	3	4	4	3	45.68	45.67	2
2	8	0	31.40	31.43	3	8	8	1	45.72	45.73	2
3	7	1	31.88	31.89	5	3	5	3	46.01	46.02	3
6	6	0	32.37	32.36	5	3	11	1	46.05	46.07	1
0	5	2	32.57	32.56	2	4	9	2	46.55	46.56	2
5	6	1	32.57	32.58	6	7	7	2	46.74	46.73	2

$a = b = 23.4646(9)$ and $c = 6.7818(5)$ with $F_{20} = 40$ (0.0135, 37).

adjacent MoO_6 octahedra. The structure of the potassium trimolybdate $K_2Mo_3O_{10}$ [18] results from the association of uncommon MoO_5 square pyramids and MoO_6 octahedra. The even less common 5-fold triangular bipyramidal coordination is observed in K_4MoO_5 [19]. This coordination is simultaneously present with the octahedral coordination in the hydrated potassium dimolybdate $K_2Mo_2O_7 \cdot H_2O$ [20], the structure of which consists of chains of edge-shared pairs of MoO_6 octahedra sharing edges with edge-shared pairs of MoO_5 trigonal bipyramids. Finally, in $Cs_4[(UO_2)_3O(MoO_4)_2(MoO_5)]$ [21] trigonal bipyramids and tetrahedral polyhedra are associated to uranyl pentagonal bipyramids to form infinite sheets $[(UO_2)_3Mo_3O_{14}]^{4-}$.

Table 3
Crystal data, intensity collection and structure refinement parameters for $K_2(UO_2)_2(MoO_4)O_2$ and $K_8(UO_2)_8(MoO_5)_3O_6$.

	$K_2(UO_2)_2(MoO_4)O_2$	$K_8(UO_2)_8(MoO_5)_3O_6$
Crystal data		
Crystal symmetry	Monoclinic	Tetragonal
Space group	$P2_1/c$	$P4/n$
Unit cell refined on powder	$a = 8.2498(9)$ Å	23.488(3) Å
	$b = 15.337(2)$ Å	23.488(3) Å
	$c = 8.3514(9)$ Å	6.7857(11) Å
	$\beta = 104.748(5)$	
	$V = 1021.8(3)$ Å^3	3743.6(9) Å^3
Z	4	4
Calculated density	$\rho = 5.27(2)$ g cm^{-3}	5.49(2) g cm^{-3}
Measured density	$\rho = 5.22(2)$ g cm^{-3}	5.44(3) g cm^{-3}
Data collection		
Temperature (K)	293(2)	293(2)
Equipment	Bruker SMART CCD	Bruker SMART CCD
Radiation Mo$K\alpha$	0.71073 Å	0.71073 Å
Scan mode	ω	ω
Recording angular range (°)	2.55–23.29	2.45–23.32
Recording reciprocal space	$-9 \leqslant h \leqslant 9$	$-26 \leqslant h \leqslant 26$
	$-17 \leqslant k \leqslant 11$	$-26 \leqslant k \leqslant 26$,
	$-9 \leqslant 1 \leqslant 9$	$-7 \leqslant 1 \leqslant 7$
No. of measured reflections	6880	
No. of independent reflections	1412	2585
μ (cm^{-1}) (for $\lambda_{K\alpha} = 0.71073$ Å)	336.74	364.36
Limiting faces and distances (mm) from an arbitrary origin	1 $\bar{1}$ 0, 0.013	1 0 0, 0.015
	$\bar{1}$ 1 0, 0.013	$\bar{1}$ 0 0, 0.015
	0 1 0, 0.070	0 1 0, 0.015
	0 $\bar{1}$ 0, 0.070	0 $\bar{1}$ 0, 0.015
	0 0 1, 0.033	0 0 1, 0.119
	0 0 $\bar{1}$, 0.033	0 0 $\bar{1}$, 0.119
R merging factor	0.056	0.052
Refinement		
Refined parameters/restraints	136/0	257/0
Goodness of fit on F^2	0.94	1.48
$R_1[I > 2\sigma(I)]$	0.046	0.055
w$R_2[I > 2\sigma(I)]$	0.102	0.099
R_1 for all data	0.069	0.060
wR_2 for all data	0.122	0.010
Largest diff. peak and hole(e Å^{-3})	3.05/−2.64	1.85/−1.68

$R_1 = \sum(|F_o| - |F_c|)/\sum|F_o|$. w$R_2 = [\sum w(F_o^2 - F_c^2)^2/\sum w(F_o^2)^2]^{1/2}$. $w = 1/[\sigma^2(F_o^2) + (aP)^2 + bP]$ where a and b are refinable parameters and $P = (F_o^2 + 2F_c^2)/3$.

Numerous other compounds of UO_3–MoO_3–M_2O ternary systems with M = Na, K, Cs, NH_4 and Ag, have been synthesized and their structures established. Phases of the binary system UO_2MoO_4–M_2MoO_4 are the most numerous and are defined by the following ratios M_2MoO_4/UO_2MoO_4: 1/6, 1/2, 1/1, 3/1, illustrated by $(NH_4)_2(UO_2)(MoO_4)_7 \cdot xH_2O$ [22–24], $Cs_2(UO_2)_2(MoO_4)_3$ [25], anhydrous $M_2(UO_2)(MoO_4)_2$ with M = Na, K, Rb [10–12] and hydrated with $2H_2O$ for M = K [11], $M_6(UO_2)(MoO_4)_4$ with M = Na, Cs [22,26]. Outside this binary line of the ternary diagram, other compounds have been also characterized, $(Na, K)_6[(UO_2)_2O(MoO_4)_4]$ [26,27] and $Rb_6[(UO_2)_2O(MoO_4)_4]$, $Rb_2[(UO_2)_6(MoO_4)_7H_2O]$….[28].

New investigations in the ternary system UO_3–MoO_3–K_2O yields to two new layered potassium uranyl molybdates $K_2(UO_2)_2(MoO_4)O_2$ and $K_8(UO_2)_8(MoO_5)_3O_6$. This paper deals with the synthesis, the single crystal structure determination and electrical conductivity measurements of these new compounds.

2. Experimental

2.1. Syntheses

Single crystals of both compounds were prepared in a K_2CO_3 flux using a mixture U_3O_8:MoO_3 of molar ratio

Table 4
Atomic coordinates and equivalent displacement parameters (Å^2) for $K_2(UO_2)_2(MoO_4)O_2$

Atom	Site	x	y	z	U_{eq} (Å^2)
U1	4*e*	0.88389(9)	0.57199(5)	0.10481(8)	0.0220(2)
U2	4*e*	0.13408(9)	0.42554(5)	0.41776(8)	0.0205(3)
Mo	4*e*	0.3781(2)	0.2623(1)	0.2103(2)	0.0241(5)
K1	4*e*	0.1739(7)	0.7644(4)	0.9244(6)	0.050(2)
K2	4*e*	0.4425(8)	0.5413(5)	0.2251(6)	0.061(2)
O1	4*e*	0.040(2)	0.6564(8)	0.123(2)	0.038(4)
O2	4*e*	0.970(2)	0.3467(9)	0.345(2)	0.026(4)
O3	4*e*	0.027(2)	0.4565(9)	0.634(1)	0.022(3)
O4	4*e*	0.101(2)	0.4645(9)	0.148(1)	0.031(4)
O5	4*e*	0.717(2)	0.4927(9)	0.097(1)	0.038(4)
O6	4*e*	0.583(2)	0.2302(9)	0.258(2)	0.036(4)
O7	4*e*	0.306(2)	0.4984(9)	0.489(2)	0.005(5)
O8	4*e*	0.337(2)	0.3340(9)	0.036(2)	0.045(5)
O9	4*e*	0.251(2)	0.169(9)	0.182(2)	0.051(5)
O10	4*e*	0.346(2)	0.3282(9)	0.372(2)	0.044(5)

Table 5
Anisotropic displacement parameters (Å^2) for $K_2(UO_2)_2(MoO_4)O_2$

Atom	U_{11}	U_{22}	U_{33}	U_{12}	U_{13}	U_{23}
U1	0.0284(6)	0.0291(5)	0.0070(4)	−0.0071(4)	0.0044(4)	−0.0007(3)
U2	0.0259(5)	0.0278(5)	0.0077(4)	−0.0025(4)	0.0064(3)	−0.0011(3)
Mo	0.0121(9)	0.0457(9)	0.0132(9)	−0.0022(9)	0.0028(7)	−0.0038(8)
K1	0.036(3)	0.101(5)	0.014(3)	0.014(3)	0.013(2)	0.019(3)
K2	0.072(5)	0.082(4)	0.016(3)	−0.055(4)	0.010(3)	−0.012(3)
O1	0.061(11)	0.022(8)	0.025(8)	−0.014(8)	0.013(8)	−0.009(6)
O2	0.028(9)	0.033(8)	0.014(7)	−0.003(7)	0.004(6)	−0.001(6)
O3	0.027(9)	0.028(8)	0.008(7)	0.004(7)	−0.005(6)	0.008(6)
O4	0.041(10)	0.035(8)	0.016(8)	−0.002(7)	0.008(7)	0.012(6)
O5	0.031(9)	0.062(9)	0.007(7)	−0.008(8)	0.001(7)	0.007(7)
O6	0.011(8)	0.073(9)	0.021(8)	0.003(8)	−0.001(6)	−0.010(8)
O7	0.008(8)	0.069(9)	0.022(8)	0.002(8)	−0.003(6)	−0.017(8)
O8	0.059(9)	0.040(9)	0.032(9)	−0.003(9)	0.018(9)	−0.003(7)
O9	0.078(9)	0.058(9)	0.019(8)	−0.034(9)	0.013(9)	−0.013(8)
O10	0.049(9)	0.054(9)	0.030(9)	−0.001(9)	0.021(8)	−0.017(8)

3:5 in a 10-fold excess of K_2CO_3. The resulting 3 g charge was thoroughly mixed and heated in a platinum crucible at 950°C during 60 h and slowly cooled at a rate of 5°C h^{-1} to room temperature. Washing of the obtained yellowish shiny crystalline product with ethanol allowed the separation of two kinds of single crystals. The yellow single crystals correspond to the $K_2(UO_2)_2(MoO_4)O_2$ phase and the orange colored single crystals belong to the $K_8(UO_2)_8(MoO_5)_3O_6$ compound. The presence of the metal elements, K, U and Mo, in both crystals was confirmed by Energy Dispersive Spectroscopy analysis performed using a JEOL JSM-5300 Scanning Microscope equipped with IMIX system of Princeton Gamma Technology (PGT).

Polycrystalline samples of $K_2(UO_2)_2(MoO_4)O_2$ and $K_8(UO_2)_8(MoO_5)_3O_6$ were prepared by conventional solid state reactions, using pure initial materials K_2CO_3 (Aldrich), U_3O_8 (Prolabo) and MoO_3 (Prolabo). Mixed starting materials in the appropriate stoichiometries were heated at 750°C in air for 2 weeks with intermediate grindings. The end of the synthesis process for each sample was controlled by X-ray powder diffraction using a Guinier-De Wolff focusing camera and Cu$K\alpha$ radiation.

Table 6
Atomic coordinates and equivalent displacement parameters (Å^2) for $K_8(UO_2)_8(MoO_5)_3O_6$

Atom	Site	Occ.	x	y	z	U_{eq} (Å^2)
U1	8*g*		0.64934(4)	0.47983(4)	0.07003(9)	0.0129(3)
U2	8*g*		0.51800(4)	0.57174(4)	0.08586(9)	0.0132(3)
U3	8*g*		0.80971(4)	0.37479(4)	0.06634(9)	0.0177(3)
U4	8*g*		0.66603(4)	0.63925(4)	0.21184(9)	0.0141(3)
Mo1	8*g*		0.78452(9)	0.51229(9)	0.2427(3)	0.0144(5)
Mo2	2*c*		3/4	3/4	0.3661(6)	0.0137(9)
Mo3	4*f*	0.5	3/4	1/4	−0.1376(9)	0.0168(9)
K1	8*g*		0.5573(3)	0.3791(3)	0.4262(9)	0.026(1)
K2	8*g*		0.5901(3)	0.5338(3)	−0.4176(9)	0.024(1)
K3	8*g*		0.7648(4)	0.6084(5)	0.7256(9)	0.057(1)
K4	8*g*		0.7146(3)	0.3980(4)	0.5670(9)	0.042(1)
O1	8*g*		0.8479(7)	0.4646(7)	0.162(3)	0.019(4)
O2	8*g*		0.7431(7)	0.4489(7)	0.141(3)	0.017(4)
O3	8*g*		0.5285(8)	0.5968(7)	−0.167(3)	0.022(4)
O4	8*g*		0.7843(9)	0.5056(8)	0.496(3)	0.029(5)
O5	8*g*		0.7214(8)	0.5564(7)	0.182(3)	0.022(4)
O6	8*g*		0.6735(7)	0.7386(7)	0.290(3)	0.016(4)
O7	8*g*		0.8077(9)	0.3948(9)	−0.190(3)	0.033(5)
O8	8*g*		0.6132(8)	0.5652(7)	0.157(3)	0.025(5)
O9	8*g*		0.8315(8)	0.5713(7)	0.181(3)	0.026(5)
O10	8*g*		0.5042(7)	0.5520(7)	0.342(3)	0.020(4)
O11	8*g*		0.6716(7)	0.5057(8)	−0.170(3)	0.024(5)
O12	8*g*		0.6766(8)	0.6541(7)	−0.048(3)	0.022(4)
O13	8*g*		0.4471(8)	0.5149(8)	0.002(3)	0.031(5)
O14	8*g*		0.6342(7)	0.4569(8)	0.322(3)	0.022(4)
O15	8*g*		0.6402(8)	0.3975(8)	−0.065(3)	0.031(5)
O16	8*g*		0.8078(9)	0.3566(9)	0.328(3)	0.036(5)
O17	8*g*		0.6575(7)	0.6278(7)	0.475(3)	0.022(4)
O18	2*c*		3/4	3/4	0.621(6)	0.035(9)
O19	8*g*		0.8220(9)	0.2750(8)	−0.004(3)	0.036(5)
O20	4*f*	0.5	3/4	1/4	−0.389(9)	0.032(9)

For each compound unit cell parameters were refined by a least-square procedure from powder X-ray diffraction data recorded at room temperature on a Siemens D5000 diffractometer using a Bragg-Brentano geometry with a back end monochromatized Cu$K\alpha$ radiation and corrected for $K\alpha_2$ contribution. The refined powder X-ray diffraction pattern data with their figures of merit F_{20}, as defined by Smith and Snyder [29], are reported in Tables 1 and 2 for $K_2(UO_2)_2(MoO_4)O_2$ and $K_8(UO_2)_8(MoO_5)_3O_6$, respectively. The densities, measured from powder samples using an automated Micromeritics Accupyc 1330 helium pycnometer using a 1-cm^3 cell, indicated $Z = 4$ formula per unit cell for the two compounds ($\rho_{mes} = 5.22(2)$ g/cm^3, $\rho_{cal} = 5.27(2)$ g/cm^3 for $K_2(UO_2)_2(MoO_4)O_2$ and $\rho_{mes} = 5.44(3)$ g/cm^3, $\rho_{cal} = 5.49(2)$ g/cm^3 for $K_8(UO_2)_8(MoO_5)_3O_6$).

Table 7
Anisotropic displacement parameters (Å^2) for $K_8(UO_2)_8(MoO_5)_3O_6$

Atom	U_{11}	U_{22}	U_{33}	U_{12}	U_{13}	U_{23}
U1	0.0131(5)	0.0145(5)	0.0110(5)	0.0002(4)	−0.0012(4)	−0.0006(4)
U2	0.0143(5)	0.0146(5)	0.0108(5)	0.0014(4)	−0.0013(4)	−0.0017(4)
U3	0.0162(5)	0.0190(5)	0.0179(5)	−0.0016(4)	0.0013(4)	0.0035(4)
U4	0.0152(5)	0.0136(5)	0.0134(5)	−0.0017(4)	−0.0008(4)	−0.0005(4)
Mo1	0.0118(11)	0.0202(12)	0.0112(12)	0.0001(9)	−0.0011(9)	0.0007(9)
Mo2	0.0121(14)	0.0121(14)	0.017(2)	0.00000	0.00000	0.00000
Mo3	0.012(3)	0.020(4)	0.018(4)	0.012(3)	0.00000	0.00000
K1	0.028(3)	0.027(3)	0.023(3)	0.002(3)	0.004(3)	0.001(3)
K2	0.026(3)	0.029(3)	0.017(3)	0.004(3)	0.002(3)	0.002(3)
K3	0.061(6)	0.074(6)	0.035(5)	0.011(4)	0.002(4)	−0.022(4)
K4	0.026(4)	0.067(5)	0.034(4)	−0.008(3)	−0.001(3)	0.024(4)
O1	0.024(10)	0.014(9)	0.019(10)	−0.007(8)	0.002(8)	−0.005(8)
O2	0.009(9)	0.026(10)	0.015(10)	0.003(8)	−0.001(7)	−0.007(8)
O3	0.037(12)	0.015(10)	0.014(10)	−0.004(8)	0.009(9)	−0.001(8)
O4	0.043(13)	0.036(12)	0.008(10)	−0.001(10)	0.004(9)	0.001(9)
O5	0.02600	0.014(9)	0.028(11)	0.011(8)	−0.006(9)	0.009(8)
O6	0.018(10)	0.011(9)	0.02(1)	0.003(7)	−0.002(8)	0.007(8)
O7	0.039(12)	0.058(14)	0.003(9)	−0.002(11)	−0.006(9)	0.008(9)
O8	0.029(11)	0.018(10)	0.029(12)	−0.006(8)	0.001(9)	0.008(9)
O9	0.025(11)	0.009(9)	0.043(13)	−0.006(8)	0.013(9)	−0.015(9)
O10	0.022(10)	0.024(10)	0.015(10)	0.007(8)	0.003(8)	0.008(8)
O11	0.016(10)	0.043(12)	0.014(10)	0.004(9)	0.001(8)	0.024(9)
O12	0.031(11)	0.021(10)	0.01400	0.012(8)	0.010(9)	0.006(8)
O13	0.028(10)	0.036(12)	0.030(12)	−0.005(9)	−0.014(9)	−0.021(9)
O14	0.021(10)	0.027(11)	0.018(10)	−0.004(8)	−0.007(8)	−0.007(9)
O15	0.028(11)	0.022(10)	0.042(13)	0.003(8)	−0.028(10)	−0.013(10)
O16	0.050(14)	0.037(13)	0.022(11)	0.010(11)	0.011(10)	0.010(9)
O17	0.022(10)	0.015(10)	0.029(12)	0.004(8)	−0.009(8)	−0.006(8)
O18	0.046(16)	0.046(16)	0.02(2)	0.00000	0.00000	0.00000
O19	0.052(14)	0.021(11)	0.03700	−0.005(9)	−0.007(11)	−0.010(9)
O20	0.001(2)	0.020(3)	0.070(4)	0.001(2)	0.00000	0.00000

2.2. Thermal analyses and conductivity measurements

Differential thermal analyses were performed in air with a SETARAM 92-1600 thermal analyzer in the temperature range 20–1000°C with heating and cooling rate 1.5°C/min using platinum crucibles. For conductivity measurements, powder samples were pelletized at room temperature and then sintered 100°C below their melting or decomposition point for 10 h resulting in a specimen of about 95% theoretical density. Gold electrodes were sputtered on both flat faces and measurements were done by impedance spectrometry in the frequency range 1–10^6 Hz using a Schlumberger 1170 frequency response analyzer. Each set of values was recorded in temperature range 200–700°C with a step of 20°C and for every measure, the temperature was stabilized during 1 h.

2.3. Crystal structures determination and refinement

The crystal structure was solved and refined for both phases from single crystal X-ray diffraction data collected on a Bruker three-circle X-ray diffractometer using graphite monochromatized Mo$K\alpha$ ($\lambda = 0.71073$ Å) radiation and equipped with a SMART charge coupled device (CCD) detector with a crystal to detector distance of 45 mm. For each single crystal, the individual frames were collected at room temperature with an omega rotation of 0.3° and 40 s count-time per frame. The reduction and correction of Lorentz, polarization and background effects were done by the program SAINTPLUS 6.02 [30]. For every single crystal, absorption corrections based on the precise crystal morphology and indexed crystal faces were applied using the program XPREP of the SHELXTL package [31] followed by SADABS program [32]. The summaries of the crystal data and details concerning the intensity data collections and structure refinements are given in Table 3.

The crystal structures of $K_2(UO_2)_2(MoO_4)O_2$ and $K_8(UO_2)_8(MoO_5)_3O_6$ were determined in the centrosymmetric $P2_1/c$ and $P4/n$ space groups, respectively, by direct methods using SHELXS program [33] which allowed the localization of the heavy atoms, U, Mo and K. The remaining anion positions were found by successively performed difference Fourier analysis calculated after refinement of the partial models. For both compounds, the final refinements were done with

Table 8
Interatomic distances (Å), valence bond and uranyl angles (°) in $K_2(UO_2)_2(MoO_4)O_2$

Atom	Distance	s_{ij}
U1–O1(i)	1.805(15)	1.603
U1–O5	1.826(15)	1.552
U1–O3(ii)	2.161(10)	0.809
U1–O4(iii)	2.218(10)	0.725
U1–O4(i)	2.393(15)	0.517
U1–O8(iii)	2.386(15)	0.532
U1–O9(iv)	2.764(16)	0.260
$\sum sij$		5.998
K1–O1(xii)	2.765(16)	0.181
K1–O1(xiii)	2.760(16)	0.183
K1–O2(xiv)	2.801(17)	0.162
K1–O6(ii)	2.812(18)	0.157
K1–O2(ii)	2.829(16)	0.152
K1–O6(xiv)	2.937(18)	0.113
K1–O3(xv)	3.353(15)	0.036
$\sum sij$		0.984
Mo–O6	1.708(16)	1.722
Mo–O9	1.752(16)	1.496
Mo–O10	1.760(17)	1.492
Mo–O8	1.787(16)	1.368
$\sum sij$		6.078
Uranyl angles (°)		
O1(i)–U1–O5	175.0(7)	
O7–U2–O2(vii)	176.6(7)	
U2–O7	1.785(15)	1.680
U2–O2(vii)	1.807(14)	1.615
U2–O3(viii)	2.222(14)	0.714
U2–O3	2.253(13)	0.678
U2–O4	2.279(10)	0.643
U2–O10	2.402(16)	0.511
U2–O9(ix)	2.613(15)	0.335
$\sum sij$		6.176
K2–O5(iii)	2.727(12)	0.199
K2–O7(ii)	2.803(17)	0.165
K2–O7	2.797(17)	0.163
K2–O5	2.839(18)	0.147
K2–O6(iv)	2.911(15)	0.122
K2–O4	2.964(17)	0.104
K2–O9(iv)	3.138(17)	0.036
$\sum sij$		0.967

Symmetry codes: (i) $1+x, y, z$; (ii) $1-x, 1-y, 1-z$; (iii) $1-x, 1-y, -z$; (iv) $1-x, 0.5+y, 0.5-z$; (v) $2-x, 1-y, -z$; (vi) $1+x, 1.5-y, -0.5+z$; (vii) $-1+x, y, z$; (viii) $-x, 1-y, 1-z$; (ix) $x, 0.5-y, 0.5+z$; (x) $-x, -0.5+y, 1.5-z$; (xi) $1-x, -0.5+y, 0.5-z$; (xii) $x, y, 1+z$; (xiii) $x, 1.5-y, 0.5+z$; (xiv) $1-x, 0.5+y, 1.5-z$; (xv) $-x, 0.5+y, 1.5-z$; (xvi) $-1+x, 1.5-y, 0.5+z$; (xvii) $x, 1.5-y, -0.5+z$; (xviii) $x, y, -1+z$; (xix) $1-x, -0.5+y, 1.5-z$; (xx) $x, 0.5-y, -0.5+z$.

anisotropic displacement parameters for all atoms. Complete lists of final atomic coordinates and anisotropic displacement parameters are given in Tables 4 and 5 and in Tables 6 and 7 for $K_2(UO_2)_2(MoO_4)O_2$ and $K_8(UO_2)_8(MoO_5)_3O_6$, respectively. The most significant inter-atomic distances with metal to oxygen bond valences and uranyl angles are reported in the Tables 8 and 9 for $K_2(UO_2)_2(MoO_4)O_2$ and $K_8(UO_2)_8(MoO_5)_3O_6$, respectively. Bond valence sums have been calculated using Brown and Altermatt data [34] with $b = 0.37$ Å except for U–O bonds where the coordination independent parameters ($R_{ij} = 2.051$ Å, $b = 0.519$ Å) were taken from Burns et al. [35].

3. Description of the crystal structures and discussion

3.1. $K_2(UO_2)_2(MoO_4)O_2$

The structure of $K_2(UO_2)_2(MoO_4)O_2$ contains two symmetrically independent uranium atoms. The two independent uranium atoms are bonded to two oxygen atoms at short distances with an average U–O bond distances of 1.82 and 1.80 Å for U(1) and U(2) atoms, respectively, to form nearly linear uranyl ions UO_2^{2+}, and to five other oxygen atoms in the equatorial plane, situated at longer distances ranging from 2.16 to 2.76 Å and from 2.22 to 2.61 Å for U(1) and U(2), respectively. Thus, the actual coordination of U atoms is a UO_7 pentagonal bipyramid. The average U–O distances for oxygen equatorial atoms (2.38 and 2.35 Å for U(1) and U(2), respectively) are in good accordance with the average value of 2.37(9) Å calculated for uranyl pentagonal bipyramids in numerous well-refined structures [35].

Four UO_7 pentagonal bipyramids are associated by two or three equatorial edges to form a cluster U_4O_{20} (Fig. 1). Within the cluster, the O(3) oxygen atoms belong to three different U atoms and correspond to the shortest U–O distances. The U_4O_{20} entities are connected by opposite O(4)–O(4) edges to form infinite two polyhedra wide ribbons, $(U_4O_{18})_\infty$, running down the [001] direction. The unique molybdenum atom is tetrahedrally coordinated with Mo–O distances ranging from 1.708(16) to 1.787(16) Å. The infinite U_4O_{18} ribbons are linked together by MoO_4 tetrahedra creating infinite layers $[(UO_2)_2(MoO_4)O_2]^{2-}$ parallel to the (100) plane, Fig. 2. A MoO_4 tetrahedron shares two vertices O(8) and O(10) with two UO_7 bipyramids that pertain to two different U_4O_{20} clusters of one ribbon and a third corner O(9) with UO_7 polyhedra of a parallel ribbon. When O(8) and O(10) are not shared between UO_7 polyhedra, the O(9) atom is shared between two UO_7 bipyramids (and a MoO_4 tetrahedron) and corresponds to the longest U–O distance in the equatorial plane of the bipyramids. The O(6) atom is not shared and gives the shortest distance to the Mo atom within the MoO_4 tetrahedron. The Mo–O bonds with the non-shared O(6) oxygen of tetrahedra connecting two consecutive ribbons are all directed towards the same side of the ribbon leading to an angle of about 90° between two consecutive ribbons. The rows of tetrahedra parallel to the [001] direction, "tip up" and "tip down", alternate leading to corrugated layers, the wave being parallel to the [010] direction, Fig. 3. It would be interesting to

Table 9
Inter-atomic distances (Å), valence bond and uranyl angles (°) in $K_8(UO_2)_8(MoO_5)_3O_6$

Atom	Distance	S_{ij}	Atom	Distance	S_{ij}	Atom	Distance	S_{ij}
U1–O11	1.815(20)	1.567	U2–O10	1.828(20)	1.546	U3–O7	1.801(20)	1.619
U1–O14	1.828(20)	1.537	U2–O3	1.831(20)	1.534	U3–O16	1.827(20)	1.537
U1–O15	2.151(19)	0.825	U2–O13	2.209(19)	0.739	U3–O15(iv)	2.092(19)	0.924
U1–O8	2.256(17)	0.672	U2–O13(i)	2.273(19)	0.652	U3–O19(v)	2.382(20)	0.529
U1–O13(i)	2.321(19)	0.594	U2–O8	2.293(19)	0.6276	U3–O1	2.382(17)	0.529
U1–O2	2.368(16)	0.542	U2–O1(iii)	2.324(17)	0.589	U3–O2	2.395(16)	0.515
U1–O5	2.584(18)	0.357	U2–O9(iii)	2.674(18)	0.302	U3–O19	2.409(19)	0.501
$\sum Sij$		6.094			5.989			6.154
U4–O12	1.814(20)	1.576	Uranyl angles (°)			K1–O7(v)	2.578(22)	0.298
U4–O17	1.817(20)	1.567	O11–U1–O14	173.8(9)		K1–O14	2.665(19)	0.237
U4–O8	2.169(17)	0.798	O10–U2–O3	175.3(9)		K1–O10(xii)	2.679(19)	0.226
U4–O9(iii)	2.338(17)	0.575	O7–U3–O16	176.7(9)		K1–O4(xiii)	2.724(22)	0.204
U4–O5	2.349(17)	0.562	O12–U4–O17	177.0(9)		K1–O3(i)	2.734(20)	0.193
U4–O6	2.399(17)	0.511				K1–O1(xiii)	2.934(21)	0.115
U4–O6(vii)	2.439(17)	0.473				K1–O16(xiii)	3.111(22)	0.071
$\sum Sij$		6.062						1.344
K2–O11	2.631(19)	0.260	K3–O12(ii)	2.794(20)	0.168	K4–O7(ii)	2.740(20)	0.193
K2–O10(viii)	2.630(19)	0.260	K3–O4	2.910(20)	0.122	K4–O16(xiii)	2.792(20)	0.169
K2–O3	2.679(20)	0.227	K3–O12(xiv)	2.925(20)	0.117	K4–O14	2.871(19)	0.135
K2–O14(viii)	2.731(20)	0.199	K3–O17	3.074(20)	0.078	K4–O16	2.893(19)	0.129
K2–O17(viii)	2.813(18)	0.158	K3–O17(vii)	3.254(22)	0.048	K4–O15(ii)	3.048(19)	0.084
K2–O8(viii)	3.028(21)	0.088	K3–O11(ii)	3.329(24)	0.040	K4–O4	3.050(19)	0.085
K2–O10(i)	3.038(18)	0.086	K3–O6(vii)	3.334(22)	0.039	K4–O2	3.199(16)	0.056
K2–O13(i)	3.166(21)	0.060	K3–O18	3.419(13)	0.031	K4–O11(ii)	3.256(20)	0.047
Sij		1.338			0.642			0.897
Mo1–O4	1.727(20)	1.627	Mo2–O18	1.730(41)	1.613	Mo3–O20	1.706(61)	1.703
Mo1–O9	1.816(20)	1.262	Mo2–O6	1.889(17)	1.053	Mo3–O19	2.007(21)	0.757
Mo1–O5	1.855(18)	1.154	Mo2–O6(iii)	1.889(17)	1.053	Mo3–O19(x)	2.007(21)	0.757
Mo1–O2	1.908(19)	1.000	Mo2–O6(ix)	1.889(17)	1.053	Mo3–O19(v)	2.032(21)	0.717
Mo1–O1	1.942(19)	0.912	Mo2–O6(vii)	1.889(17)	1.053	Mo3–O19(iv)	2.032(21)	0.717
$\sum Sij$		5.955			5.825			4.651
Mo3–Mo3(iv)	1.867(9)		O20–O20(xvi)	1.51(9)				

Symmetry codes: (i) $1-x, 1-y, -z$; (ii) $x, y, 1+z$; (iii) $y, 1.5-x, z$; (iv) $0.5+y, 1-x, -z$; (v) $1-y, -0.5+x, -z$; (vi) $0.5+y, 1-x, 1-z$; (vii) $1.5-y, x, z$; (viii) $x, y, -1+z$; (ix) $1.5-x, 1.5-y, z$; (x) $1.5-x, 0.5-y, z$; (xi) $1.5-x, 0.5-y, -1+z$; (xii) $1-x, 1-y, 1-z$; (xiii) $1-y, -0.5+x, 1-z$; (xiv) $1.5-y, x, 1+z$; (xv) $y, 1.5-x, -1+z$; (xvi) $0.5+y, 1-x, -1-z$.

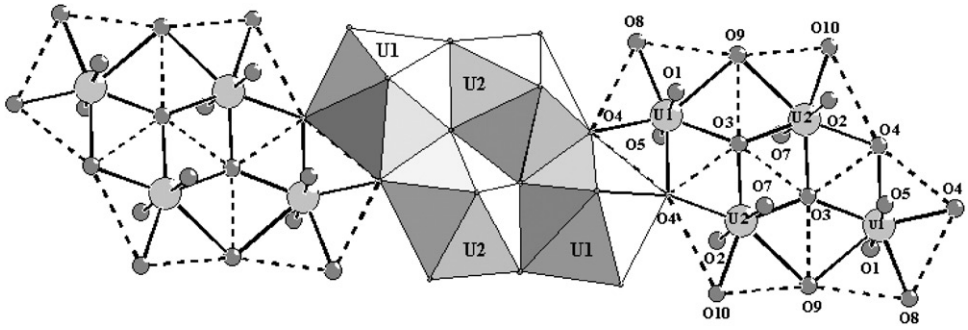

Fig. 1. The infinite two pentagonal bipyramids wide (U_4O_{18}) ribbon running down [001] in $K_2(UO_2)_2(MoO_4)O_2$.

synthesize materials built on the same association of polyhedra in which the rows of tetrahedra up and down does not alternate, so square columnar structure should be obtained. The corrugated layers are stacked along the [100] direction and the potassium ions are located between the layers and hold them together, Fig. 3. Similar one-dimensional two polyhedra wide ribbons built from edge-sharing pentagonal bipyramids have been described in the hydrated calcium uranyl oxide $Ca[(UO_2)_4O_3(OH)_4](H_2O)_2$ [36]. In this compound the double chains are connected together by other two polyhedra wide ribbons in which half of the pentagonal bipyramids are replaced by distorted square bipyramids, leading to sheets of uranium polyhedra. Discrete

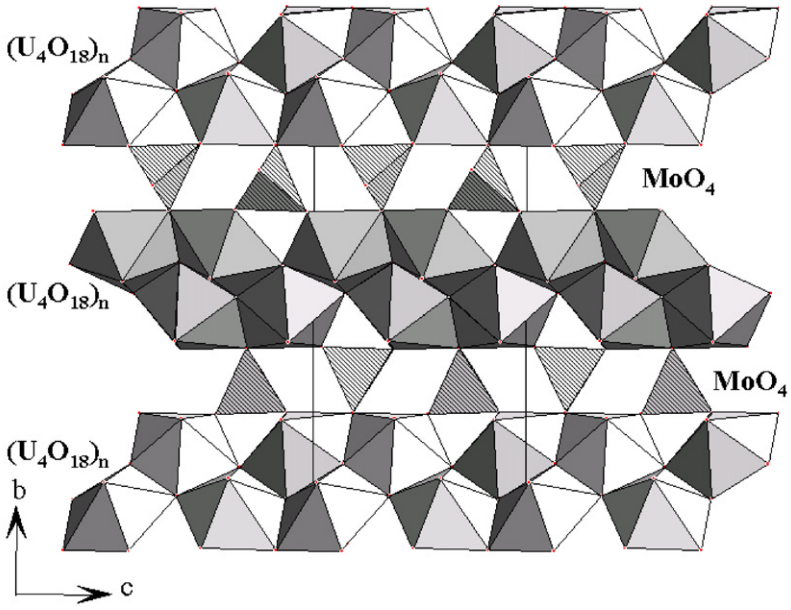

Fig. 2. Projection on the (100) plane of the undulated layer $[(UO_2)_2(MoO_4)O_2]^{2-}$ of the $K_2(UO_2)_2(MoO_4)O_2$ compound resulting from the connection of (U_4O_{18}) ribbons by MoO_4 tetrahedra.

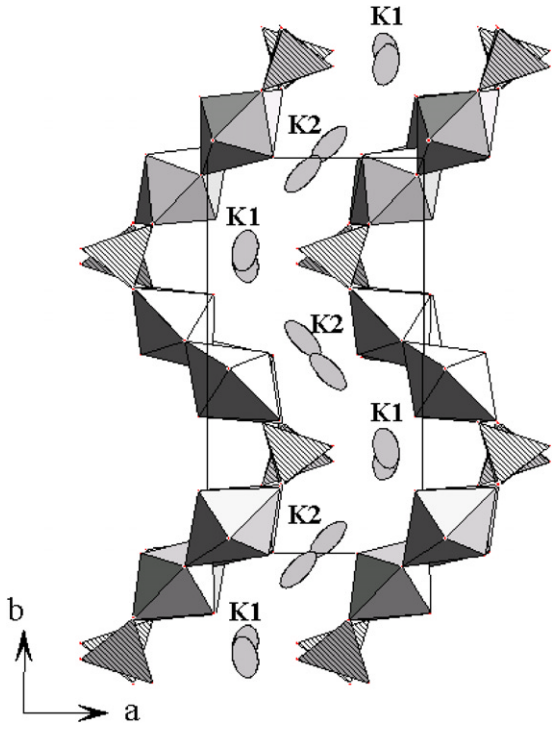

Fig. 3. Projection of the crystal structure of $K_2(UO_2)_2(MoO_4)O_2$ on the (001) plane showing the corrugated $[(UO_2)_2(MoO_4)O_2]^{2-}$ layers stacked along the *a*-axis and the interlayer K atoms.

tetranuclear complexes isotypic to U_4O_{20} in which chloride and hydroxyl anions, or water molecules, are substituted for oxygen atoms are observed in other compounds such as $[(UO_2)_4Cl_2O_2(OH)_2(H_2O)_6](4H_2O)$ [37], $K_2[(UO_2)_4O_2(OH)_2Cl_4(H_2O)_4](2H_2O)$ [38] and $M_4[(UO_2)_4Cl_8O_2(H_2O)_2](2H_2O)$ with M = Rb and Cs [39], in these compounds the isolated clusters $U_4(O, Cl, OH, OH_2)_{20}$ are linked together only by water molecules in the first compound, and by alkali atoms and H_2O molecules in the two others.

The two symmetrically distinct interlayer K atoms are coordinated to 7 oxygen atoms at distances ranging from 2.727(12) to 3.353(15) Å. Bond valence sums calculation for metals (Table 8) confirms the valence of +6 for all U and Mo atoms and +1 for K atoms, with 5.998, 6.176, 6.078, 0.984 and 0.967 vu for U(1), U(2), Mo, K(1) and K(2), respectively. For oxygen atoms the calculated bond valence sums range from 1.853 to 2.158 vu with an average value of 2.003 vu.

3.2. $K_8(UO_2)_8(MoO_5)_3O_6$

There are 31 unique atoms (4 U, 3 Mo, 4 K and 20 O) in $K_8(UO_2)_8(MoO_5)_3O_6$, all of which occupy general (8*g*) positions except two molybdenum and two oxygen atoms, which are in special (4*f*) and (2*c*) sites. The special (4*f*) positions for the molybdenum Mo(3) and oxygen O(20) atoms are half occupied. As being observed in almost all the uranyl compounds the four symmetrically independent U^{VI} cations are part of approximately linear UO_2^{2+} uranyl ions, the uranyl ions are coordinated by five oxygen atoms arranged at the equatorial corners of pentagonal bipyramids. Although acceptable, the averages of the uranium–equatorial oxygen distances (2.34, 2.35, 2.33 and 2.33 Å for U(1), U(2), U(3) and U(4), respectively) are rather weak compared with the mean value of 2.37(9) [35], on the contrary the bond-lengths within the uranyl ions are rather long, however the bond valence sums are

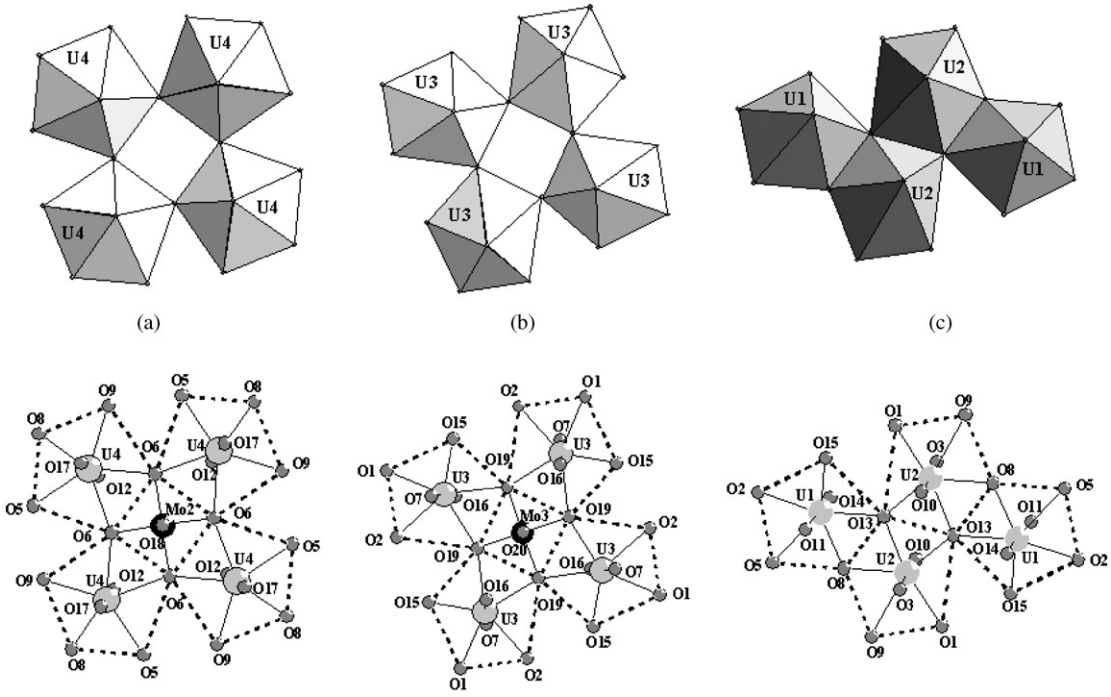

Fig. 4. The different uranyl molybdate clusters considered as the building blocks of the layered structure of $K_8(UO_2)_8(MoO_5)_3O_6$, (a) $U(3)_4O_{25}$, (b) $U(4)_4O_{25}$ and (c) $U(1)_2\ U(2)_2O_{24}$.

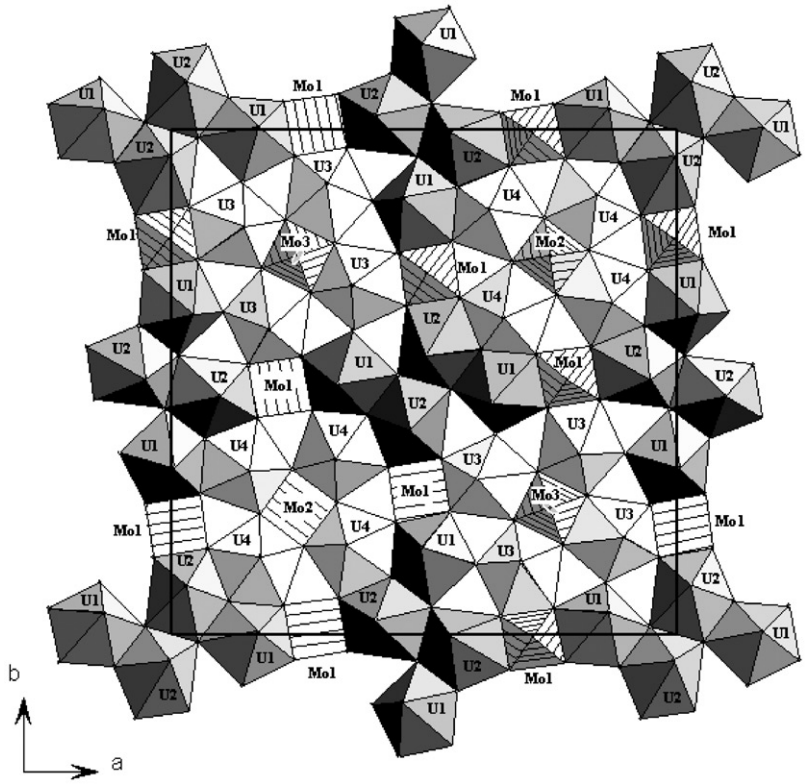

Fig. 5. Projection of the infinite sheet $[(UO_2)_8(MoO_5)_3O_6]^{8-}$ on the (001) plane of the $K_8(UO_2)_8(MoO_5)_3O_6$ compound, showing the bidimensional arrangement of UO_7 pentagonal bipyramids and MoO_5 square pyramids.

perfectly in agreement with the oxidation degree +6 of the uranium. Four $U(4)O_7$ pentagonal bipyramids related by the 4-fold axis are connected by O(6) equatorial corners to form a U_4O_{24} entity (Fig. 4a). In the same way, four $U(3)O_7$ pentagonal bipyramids related by the inversion tetrad axis are connected by

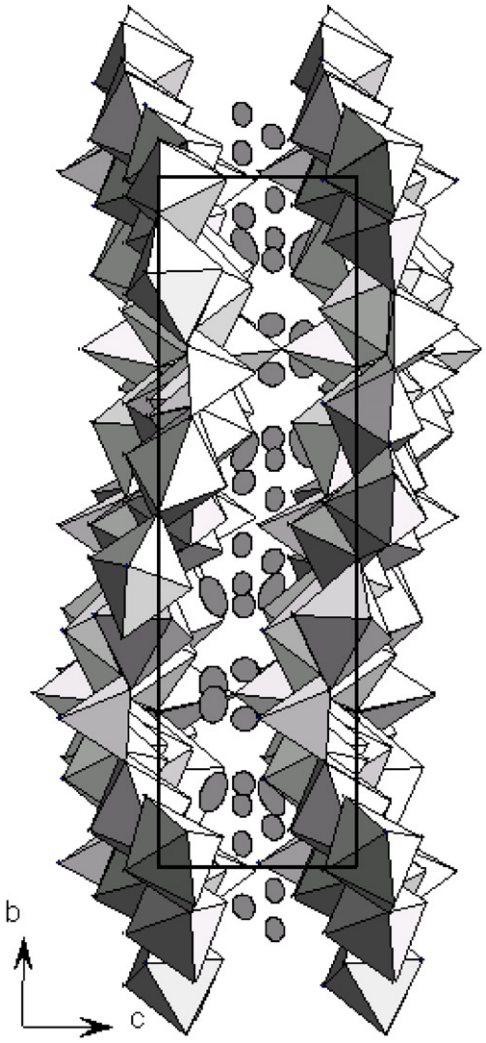

Fig. 6. The staking of the $[(UO_2)_8(MoO_5)_3O_6]^{8-}$ layers in the $K_8(UO_2)_8(MoO_5)_3O_6$ compound with the K^+ ions in the interspace.

O(19) equatorial corners to form an other U_4O_{24} entity (Fig. 4b). Finally two U(2)O_7 polyhedra related by an inversion center shared an O(13)–O(13) edge to form a dimeric unit that share its two O(13)–O(8) edges with two U(1)O_7 bipyramids to constitute a dense tetranuclear U_4O_{22} entity. Each polyhedron of the $U(4)_4O_{24}$ moiety shares its two O(5)–O(8) and O(8)–O(9) edges with one U_4O_{22} entity and the $U(3)_4O_{22}$ moieties share all their equatorial corners with four U_4O_{22} entities to form corrugated sheets parallel to (001) plane (Fig. 5). The so-obtained U_8O_{37} sheet creates triangular, square and pentagonal holes. The pentagonal holes can be described as a quadrangular site flanked by a triangular one. All the triangular sites are unoccupied, on the contrary all the square sites are occupied by molybdenum atoms, the coordination of each Mo atom being completed by a fifth oxygen to form a square pyramid. Each molybdenum atom is strongly bonded to the apical oxygen atom of the square pyramidal polyhedron which corresponds to oxygen non-shared with the UO_7 bipyramids, with the shortest Mo–O bond lengths ranging from 1.706(61) to 1.730(41) Å. The square equatorial oxygen atoms are less bonded to Mo atoms with average distances 1.880, 1.889 and 2.019 for Mo(1), Mo(2) and Mo(3), respectively. Mo(2) is above the center of the $U(4)_4O_{24}$ entity, the axial Mo(2)–O(18) bond is on the 4-fold axis and the four Mo(2)–O(6) distances are equal. The Mo(3) atom is above the center of the $U(3)_4O_{24}$ entity, the axial Mo(3)–O(20) bond is on the $\bar{4}$-fold axis, the equatorial Mo(3)–O(19) distances are longer than the values generally observed for Mo in square pyramidal coordination and for the Mo(1) and Mo(2). In fact the Mo(3) atom is more away from the oxygen equatorial plane (0.93 Å instead of 0.51 Å for Mo(1) and Mo(2)), this can result from the disorder affecting Mo(3) and O(20) atoms and explains the underbonding of the Mo(3) atom (calculated valence bond sum = 4.65 vu).

The potassium ions are located in the interlayer spaces between the sheets $[(UO_2)_8(MoO_5)_3O_6]^{8-}$ resulting from the linkage of the UO_7 pentagonal bipyramids and MoO_5 square pyramids, Fig. 6. In this compound, there are five types of oxygen atoms, oxygens of (i) the UO_2^{2+} uranyl ions and (ii) the strong apical Mo–O bond, the corresponding U–O and Mo–O bonds are directed towards the interspace and the oxygen atoms participate to the coordination of K, (iii) oxygen atoms of the equatorial plane of the MoO_5 pyramids which are shared to two UO_7 bipyramids and lead to the longest U–O distances ranging from 2.324(17) to 2.674(18) Å, (iv) O(8) and O(13) shared between three UO_7 bipyramids and thus are at the center of U_3 triangles and correspond to intermediate U–O distances ranging from 2.169(17) to 2.321(19) Å, and (v) O(15) shared between only two UO_7 bipyramids and giving the shortest U–O equatorial distances of 2.151(19) and 2.092(19) Å for U(1) and U(3), respectively.

3.3. Thermal stability

DTA measurements showed that $K_2(UO_2)_2(MoO_4)O_2$ congruently melts at 930°C, while for $K_8(UO_2)_8(MoO_5)_3O_6$ the melting occurs at 940°C. The powder X-ray diffraction analyses of residues after each DTA measurement, confirm the existence of the starting single phase for the first compound, while for $K_8(UO_2)_8(MoO_5)_3O_6$ two phases system is observed, $K_2(UO_2)_2(MoO_4)O_2$, and $K_2U_2O_7$, so decomposition occurs according the reaction:

$$K_8(UO_2)_8(MoO_5)_3O_6 \rightarrow 3K_2(UO_2)_2(MoO_4)O_2 + K_2U_2O_7$$

immediately followed by the melting of $K_2(UO_2)_2(MoO_4)O_2$ compound.

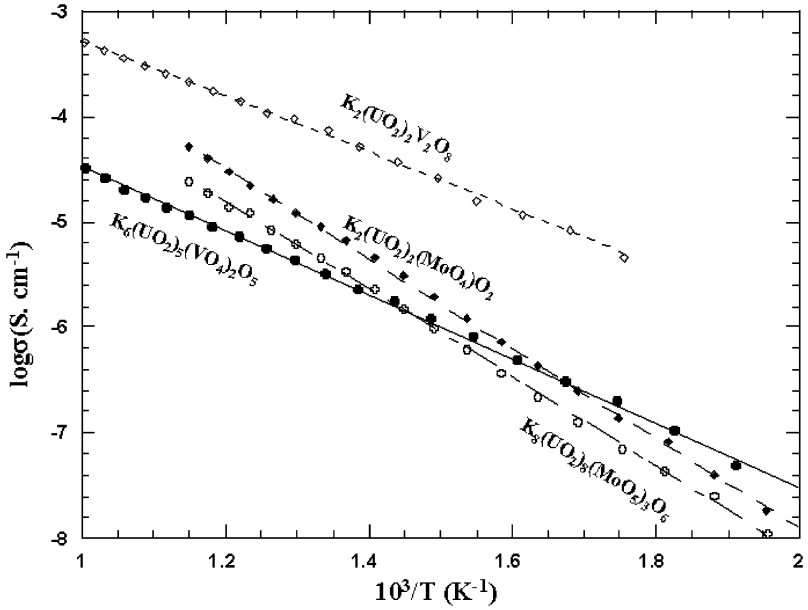

Fig. 7. Comparison between potassium uranyl molybdates and potassium uranyl vanadates conductivity vs temperature.

Table 10
Specific conductivity at 600°C and activation energy of some potassium uranyl compounds

Compound	σ ($S\,cm^{-1}$) × 104	E_a (eV)
$K_8(UO_2)_8(MoO_5)_3O_6$	0.24	0.86
$K_2(UO_2)_2(MoO_4)O_2$	0.52	0.87
$K_6(UO_2)_5(VO_4)_2O_5$	0.11	0.56
$K_2(UO_2)_2V_2O_8$	2.51	0.57

3.4. Electrical properties

The layered structure of $K_2(UO_2)_2(MoO_4)O_2$ and $K_8(UO_2)_8(MoO_5)_3O_6$ compounds with relatively large K displacement parameters allow us to consider some mobility of the alkaline cations localized between layers. Fig. 7 indicates the temperature dependence of the conductivity for the two compounds, for comparison conductivity variations for two other already studied K-uranyl vanadates $K_2(UO_2)_2V_2O_8$ (40) and $K_6(UO_2)_5(VO_4)_2O_5$ [41] are also reported. The conductivity measurements show that the ionic conductivity obeys to the Arrhenius law over the studied temperature range, with a linear evolution of log σ according to $1/T$. The two studied compounds exhibit comparable conductivity and the same activation energy higher than those of the vanadates compounds (Table 10). Fig. 3 shows that the vibration of both K(1) and K(2) atoms in $K_2(UO_2)_2(MoO_4)O_2$ is basically along the undulation direction of the layers, thus the two cations could be responsible of the observed conductivity. In $K_6(UO_2)_5(VO_4)_2O_5$ the layers are less corrugated and the activation energy lower. In $K_8(UO_2)_8(MoO_5)_3O_6$, K(3) and K(4) have higher displacement parameters than K(1) and K(2) and are underbonded, so they are probably the mobile species, however the mobility is limited by the blocking of the interspace, particularly by some apical Mo–O bonds. Finally the best K-conductor of the series remains the carnotite type compound $K_2(UO_2)_2V_2O_8$ [40] in which the layers are flat and the K atoms underbonded.

References

[1] P.C. Burns, R. Finch, (Eds.), Rev.Minerol. 38 (1999) 23.
[2] J. Benavente, J.R. Ramos-Barrado, M. Martinez, S. Bruque, J. Appl. Electrochem. 25 (1995) 68.
[3] J.C. Boivin, C. Pirovano, G. Nowogrocki, G. Mairesse, Ph. Labrune, G. Lagrange, Solid State Ion. 113–115 (1998) 639.
[4] L.M. Kovba, V.K. Trunov, A.J. Grigorev, Zh. Strukt. Khim. 6 (1965) 919.
[5] V.N. Serezhkin, V.V. Tabachenko, L.B. Serezhkina, Radiokhimiya 20 (1978) 214.
[6] V.N. Serezhkin, L.M. Kovba, V.K. Trunov, Kristallografiya 17 (6) (1972) 1127.
[7] V.N. Serezhkin, L.M. Kovban, L.G. Makarevich, Kristallografiya 25 (1980) 858.
[8] I. Linquist, Acta Chem. Scand. 4 (1950) 1066.
[9] B.M. Gatehouse, P. Leverett, J. Chem. Soc. A (1950) 1066.
[10] S.V. Krivovichev, R.J. Finch, P.C. Burns, Can. Mineral. 40 (2002) 193.
[11] G.G. Sadikov, T.I. Krasovskaya, Y.A. Polyakov, V.P. Nikolaev, Neorg. Mater. 24 (1) (1998) 109.
[12] E.A. Tatarinova, L.B. Serezkhin, V.N. Serezkhin, Radiokhimiya 33 (3) (1991) 61.
[13] S.V. Krivovichev, P.C. Burns, Can. Mineral. 38 (2000) 717.
[14] V.N. Serezkhin, V.F. Chuvaev, L.M. Kovba, V.K. Trunov, Dokl. Akad. Nauk SSSR. 210 (1973) 873.
[15] S.V. Krivovichev, P.C. Burns, Can. Mineral. 38 (2000) 847.

[16] B.M. Gatehouse, P. Leverett, J. Chem. Soc. D (1970) 740.
[17] M. Seleborg, Act. Chem. Scand. 21 (1967) 499.
[18] B.M. Gatehouse, P. Leverett, J. Chem. Soc. A (1968) 1398.
[19] T. Betz, R. Hoppe, J. Less-Common Met. 105 (1985) 87.
[20] B.M. Gatehouse, A.J. Jozsa, J. Solid State Chem. 71 (1987) 34.
[21] S.V. Krivovichev, P.C. Burns, Can. Mineral. 40 (2002) 201.
[22] I. Duribreux, Thesis, Lille, 1997.
[23] G.G. Tabachenko, L.M. Kovba, V.N. Serezkhin, Koord. Khim. 10 (1983) 558.
[24] S.V. Krivovichev, P.C. Burns, Can. Mineral. 39 (2001) 207.
[25] S.V. Krivovichev, C.L. Cahill, P.C. Burns, Inorg. Chem. 41 (2002) 34.
[26] S. Obbade, C. Dion, M. Saadi, F. Abraham, 31èmes Journées des Actinides, Saint-Malo, France 26–28 April 2001, Extended abstracts, O7 and P5.
[27] S.V. Krivovichev, P.C. Burns, Can. Mineral. 39 (2001) 197.
[28] S.V. Krivovichev, P.C. Burns, J. Solid State Chem. 168 (2002) 245.
[29] G. Smith, R.J. Snyder, J. Appl. Crystallogr. 12 (1979) 60.
[30] SAINT Plus version 5.00, Bruker Analytical X-ray Systems , Madison, WI, 1998.
[31] G.M. Sheldrick, SHELXTL NT, Program Suite for solution and Refinement of Crystal Structure version 5.1, Bruker Analytical X-ray Systems, Madison, WI, 1998.
[32] R.H. Blessing, SADAPS: program for absorption correction using SMART CCD based on the method of blessing, Acta Crystallogr. A51 (1995) 33.
[33] G.M. Sheldrick, Acta Crystallogr. A46 (1990) 467.
[34] I.D. Brown, D. Altermatt, Acta Crystallogr. B 41 (1985) 244.
[35] P.C. Burns, R.C. Ewing, F.C. Hawthorne, Can. Mineral. 35 (1997) 1551.
[36] R.E. Glatz, Y. Li, K.A. Hughes, C.L. Cahill, P.C. Burns, Can. Mineral. 40 (2001) 217.
[37] M. Åberg, Acta Chem. Scand. A30 (1976) 507.
[38] A. Perrin, J.Y. Le Marouille, Acta Crystallogr. B33 (1977) 2477.
[39] A. Perrin, J. Inorg. Nucl. Chem. 39 (1977) 1169.
[40] F. Abraham, C. Dion, M. Saadi, J. Mter. Chem. 3 (5) (1993) 459.
[41] C. Dion, S. Obbade, E. Raekelboom, F. Abraham, J. Solid State Chem. 155 (2000) 342.